Alexandria Engineering Journal (2016) xxx, xxx–xxx

HOSTED BY

ELSEVIER

Alexandria University

Alexandria Engineering Journal

www.elsevier.com/locate/aej
www.sciencedirect.com

ORIGINAL ARTICLE

# Magnetohydrodynamic Cattaneo-Christov flow past a cone and a wedge with variable heat source/sink

**K. Anantha Kumar [a], J.V. Ramana Reddy [a], V. Sugunamma [a,*], N. Sandeep [b,*]**

[a] *Department of Mathematics, Sri Venkateswara University, Tirupati 517502, A.P., India*
[b] *Department of Mathematics, VIT University, Vellore 632014, Tamil Nadu, India*

Received 31 August 2016; revised 4 November 2016; accepted 6 November 2016

**KEYWORDS**

MHD;
Non-uniform heat source/sink;
Cattaneo-Christov heat flux;
Cone and wedge

**Abstract** In the present article, the problem of boundary layer flow of MHD electrically conducting fluid past a cone and a wedge with non-uniform heat source/sink along with Cattaneo-Christov heat flux is investigated numerically. At first, the flow equations are converted into ODE via appropriate self similarity transforms and the resulting equations are solved with the assistance of R.-K. and Newton's methods. The influence of several dimensionless parameters on velocity and temperature fields in addition to the friction factor and reduced heat transfer coefficient has been examined with the support of graphs and numerical values. The heat transfer phenomenon in the flow caused by the cone is excessive when compared to the wedge flow. Also, the thermal and momentum boundary layers are not the same for the flow over a cone and wedge.



## 1. Introduction

The boundary layer flow of a viscous electrically conducting fluid over a wedge in the presence of Lorentz force has magnetized the attention of many authors owing to its significance in technology and science such as oil exploration, nuclear reactors, plasma studies, MHD generators and boundary layer control in aerofoil. By keeping a view into these, Stewart and Prober [1], and Lin and Lin [2] described the impact of heat transfer on the boundary layer flow caused by a wedge. Vajravelu and Nayfeh [3] numerically investigated the influence of heat generation on the MHD flow along the surface of a cone. In continuation of this, Chamkha [4] analysed the flow past a cone and wedge through porous medium. He found that a rise in Darcy number enhances the friction factor. The impact of thermal radiation on the boundary layer flow of a non-Newtonian liquid along a wedge was reported by Hsu et al. [5]. Yih [6] presented a mathematical model to examine the impact of suction/blowing on laminar flow through a wedge. Then after, Kumari [7] investigated the effects of adequate blowing rates and induced magnetic field on the wedge flow. The influence of applied magnetic field on mixed convective flow past a wedge under the influence of viscous dissipation was studied by Kumari et al. [8]. Massoudi [9] has found a new mathematical model to discuss the heat transfer of the power-law fluid past a wedge considering heat genera-

* Corresponding authors.
E-mail addresses: vsuguna@svuniversity.ac.in (V. Sugunamma), nsreddy.dr@gmail.com (N. Sandeep).

Peer review under responsibility of Faculty of Engineering, Alexandria University.

http://dx.doi.org/10.1016/j.aej.2016.11.013

**Nomenclature**

| | |
|---|---|
| $A^*$ | non-uniform heat source or sink parameter |
| $a$ | constant |
| $B^*$ | non-uniform heat source or sink parameter |
| $B_0$ | applied magnetic field strength |
| $C_f^*$ | dimensional wall shear stress |
| $C_f$ | friction factor |
| $c_p$ | specific heat at constant pressure |
| $Gr$ | Grashof number |
| $g$ | acceleration due to gravity |
| $h$ | heat transfer coefficient |
| $k$ | thermal conductivity |
| $l$ | characteristic length |
| $M$ | magnetic field parameter |
| $Nu$ | Nusselt number |
| $Pr$ | Prandtl number |
| $r$ | radius of the cone |
| $s$ | wall temperature parameter |
| $T$ | temperature of the fluid |
| $T_w$ | temperature near the surface |
| $T_\infty$ | ambient temperature |
| $u, v$ | velocity components along $x$ and $y$ directions respectively |
| $u_w$ | velocity near the flow surface |

*Greek letters*

| | |
|---|---|
| $\beta$ | thermal relaxation parameter |
| $\beta_T$ | volumetric thermal expansion coefficient |
| $\delta$ | relaxation time of heat flux |
| $\Omega$ | wedge full angle |
| $\gamma$ | cone/wedge half angle |
| $\xi$ | stream function |
| $\mu$ | dynamic viscosity |
| $\upsilon$ | kinematic viscosity |
| $\rho$ | density of the fluid |
| $\sigma$ | electrical conductivity of the fluid |
| $\zeta$ | similarity variable |

tion. By making use of Runge-Kutta Gill method, the impact of chemical reaction and Joule's dissipation on the wedge flow was discussed by Devi and Kandasamy [10]. Cheng and Lin [11] investigated the Falkner-Skan wedge flow by taking into consideration heat flux and wall temperature.

Kim [12] presented an analytical solution to study the time dependent convective transport of a micropolar fluid. The effects of heat transfer on the flow caused by a wedge with first order chemical reaction were numerically analysed by Kandasamy et al. [13]. An analytical solution to investigate the asymmetric flow over a stretched surface using Kummer's function was presented by Ouaf [14] and concluded that increasing values of wall temperature parameter suppress the fluid temperature. The heat transfer of unsteady mixed convective flow past a symmetric wedge was deliberated by Hossain et al. [15]. The influences of heat source/sink and chemical reaction on the flow of viscous micropolar fluid past a cone with magnetic field were studied by El-Kabeir et al. [16] and stated that increasing values of magnetic field parameter suppress the fluid motion. Yao [17] has given a strange mathematical model to analyse the flow past a wedge using Falkner-Skan model. On the other hand a mathematical model was constructed by Hayat et al. [18] and Postelnicu and Pop [19] to discuss the flow properties of non-Newtonian fluids along a wedge. In continuation of this, Seddeek et al. [20] discussed the influence of varying thermal conductivity on the wedge flow by using Keller box technique. Similar type of study on nanofluids was presented by Yacob et al. [21]. The influence of heat flux and the magnetic field on the convective flow past a wedge was investigated by Rashad and Bakier [22]. Atalik and Sonmezler [23] studied the significance of electric field on the flow induced by a wedge.

Hsiao [24] has considered the study of second grade fluid flow over a porous wedge. Rahman et al. [25] analysed the effects of heat source/sink on MHD nanofluid flow over a wedge with convective surface. Through this study, they found that velocity of the nanofluid enhances with elevating values of wedge angle. The impact of linear radiation on a chemically reacting flow with nanoparticles along a moving wedge was examined by Khan et al. [26]. Kandasamy et al. [27] worked on unsteady motion of a nano liquid along a wedge by taking solar radiation and viscous dissipation. An investigation on the problem of mixed convective flow past a wedge with porous medium was done by Rashidi et al. [28]. Kasmani et al. [29] explored the effects of thermophoresis and Brownian motion on the wedge flow. The effects of Lorentz force and non-uniform heat on the flow caused by a slendering sheet were inquired by Ramana Reddy et al. [30]. Mathili et al. [31] studied the impact of higher order chemical reaction on Casson fluid flow caused by a cone with heat absorption. In this study, they found that the heat generation helps to elevate the fluid velocity. Babu et al. [32] considered the study of Eyring-Powell fluid flow caused by a cone with heat transfer. Raju and Sandeep [33] presented the dual solutions to analyse the bio-convective flow of Williamson fluid past two different geometries namely cone and plate. A numerical analysis on the flow over a wedge and a cone with thermal radiation was performed by Harbi [34] by employing finite difference method.

The heat conduction law suggested by Fourier [35] was utilized by many authors to picture the heat transfer phenomenon. Further, this model was amended by Cattaneo [36] by including relaxation time. In continuation of this, Christov [37] proposed a derivative model of Cattaneo's law and that became popular as Cattaneo-Christov heat flux model. This mechanism plays a pivotal role in medical and bio-engineering processes such as reducing heat in nuclear reactors, hybrid power generators, electronic devices and pasteurization of milk. Owing to these numerous applications in heat transfer mechanism, many researchers are using this model in their studies. Among them Han et al. [38] and Hayat et al. [39] addressed the heat transfer behaviour of Maxwell fluid past a stretched sheet using Cattaneo-Christov heat flux model. Further, this model was extensively used by many researchers [40–42] to construct the energy equation and discussed the flow and heat transfer behaviour of various kinds of non-Newtonian fluids. In addition to these, the authors [43–46] have been giving importance in their research to illustrate the MHD flow of different types of non-Newtonian fluid

Please cite this article in press as: K. Anantha Kumar et al., Magnetohydrodynamic Cattaneo-Christov flow past a cone and a wedge with variable heat source/sink, Alexandria Eng. J. (2016), http://dx.doi.org/10.1016/j.aej.2016.11.013

flows with Cattaneo-Christov heat flux. Shehzad et al. [47] inquired the impact of nonlinear convection on Oldroyd-B fluid using the same heat flux model. Abbasi and Shehzad [48] applied the Cattaneo-Christov heat flux model to inspect the three-dimensional flow of non-Newtonian fluid across a bidirectional surface. The studies [49,50] also dealt with the boundary layer flow of Oldroyd-B fluid. Shehzad et al. [51] utilized the same heat flux theory to execute the study of 2D third-grade fluid flow.

The major objective of the present work was to analyse the impact of heat flux model proposed by Cattaneo-Christov on the flow over a wedge and a cone. The impact of non-uniform heat source or sink is also considered. The transformed boundary layer equations of the flow are solved by using R.K. and Newton's methods. Further, the influence of pertinent parameters such as magnetic field parameter, thermal Grashof number, wall temperature parameter, thermal relaxation parameter, Prandtl number and non-uniform heat parameters on velocity and temperature fields along with friction factor and reduced Nusselt number are examined and shown in graphs and tables. Finally a comparison of the current work with the earlier results [52] is also made for the purpose of validating the results.

## 2. Mathematical formulation

We supposed a steady, incompressible, free convective laminar flow of a fluid over two different geometries (cone and wedge). The flow is supposed to be electrically conducting. The coordinate system is considered in such a way that $x$-axis coincides with the surface of the flow geometry, and $y$-axis measures the orthogonally outward to it. A transverse magnetic field of strength $B_0$ is applied orthogonal to the surface of the geometries as depicted in Fig. 1. Suppose that $\gamma$ is the half angle of the cone, $\Omega$ is the wedge full angle and $r$ is radius of the cone. The temperature near the surface is considered as $T_w = T_\infty + ax^s$, where $a$ is a constant, $s$ is the wall temperature parameter (the temperature at the wall is constant when $s = 0$), $T_\infty$ is the ambient temperature. Cattaneo-Christov heat flux is taken into account. Induced magnetic field and viscous dissipation are ignored in this analysis.

As per the afore mentioned restrictions, the partial differential equations that govern the flow in terms of stream function $\xi$ can be expressed as (see [30,31,45,46])

$$\frac{\partial}{\partial x}\left(r^m\frac{\partial \xi}{\partial y}\right)-\frac{\partial}{\partial y}\left(r^m\frac{\partial \xi}{\partial x}\right)=0, \tag{1}$$

$$\frac{\partial \xi}{\partial y}\frac{\partial^2 \xi}{\partial x\partial y}-\frac{\partial \xi}{\partial x}\frac{\partial^2 \xi}{\partial y^2}=\upsilon\frac{\partial^3 \xi}{\partial y^3}+g\beta_T(T-T_\infty)\cos\gamma-\frac{\sigma B_0^2}{\rho}\frac{\partial \xi}{\partial y}, \tag{2}$$

$$\begin{aligned}\frac{\partial \xi}{\partial y}\frac{\partial T}{\partial x}-\frac{\partial \xi}{\partial x}\frac{\partial T}{\partial y}&=\frac{k}{\rho c_p}\frac{\partial^2 T}{\partial y^2}+\frac{q'''}{\rho c_p}\\&-\delta\left(\frac{\partial \xi}{\partial y}\frac{\partial^2 \xi}{\partial x\partial y}\frac{\partial T}{\partial x}+\frac{\partial \xi}{\partial x}\frac{\partial^2 \xi}{\partial y\partial x}\frac{\partial T}{\partial y}-\frac{\partial \xi}{\partial y}\frac{\partial^2 \xi}{\partial x^2}\frac{\partial T}{\partial y}-\frac{\partial \xi}{\partial x}\frac{\partial^2 \xi}{\partial y^2}\frac{\partial T}{\partial x}\right.\\&\left.-2\frac{\partial \xi}{\partial y}\frac{\partial \xi}{\partial x}\frac{\partial^2 T}{\partial x\partial y}+\left(\frac{\partial \xi}{\partial y}\right)^2\frac{\partial^2 T}{\partial x^2}+\left(\frac{\partial \xi}{\partial x}\right)^2\frac{\partial^2 T}{\partial y^2}\right),\end{aligned} \tag{3}$$

The corresponding boundary conditions are

$$\begin{aligned}&\xi_y(x,0)=u_w=\upsilon x l^{-2},\quad -\xi_x(x,0)=0,\\&T(x,0)=T_w=T_\infty+ax^s,\\&\xi_y(x,\infty)=0,\quad T(x,\infty)=T_\infty,\end{aligned} \tag{4}$$

The proposed problem shows two-different geometries based on the following assumptions:

(i) $m = 0$ and $\gamma \neq 0$: Flow caused by a wedge.
(ii) $m = 1$ and $\gamma \neq 0$: Flow caused by a cone.

where the velocity components along $x$ and $y$ directions have velocities $u=\frac{\partial \xi}{\partial y}$ and $v=\frac{-\partial \xi}{\partial x}$ respectively.

In Eq. (3) $q'''$ is the non-uniform heat source or sink given by (see [30])

$$q'''=\frac{k u_w(x)}{x\upsilon}[A^*(T_w(x)-T_\infty)f'+B^*(T-T_\infty)], \tag{5}$$

Here $A^* > 0$, $B^* > 0$ represent heat generation in the flow and $A^* < 0$, $B^* < 0$ denote absorption of the same.

Eqs. (1)–(4) are in dimensional form. In order to make them dimensionless, we use the following similarity transformations.

$$\zeta=\frac{y}{l},\quad u=\frac{\upsilon x}{l^2}\frac{\partial f}{\partial \zeta},\quad v=\frac{-\upsilon(m+1)}{l}f(\zeta),$$
$$T=T_\infty+(T_w-T_\infty)\theta(\zeta),$$

Now substituting the above similarity transformations in Eqs. (1)–(3), gives

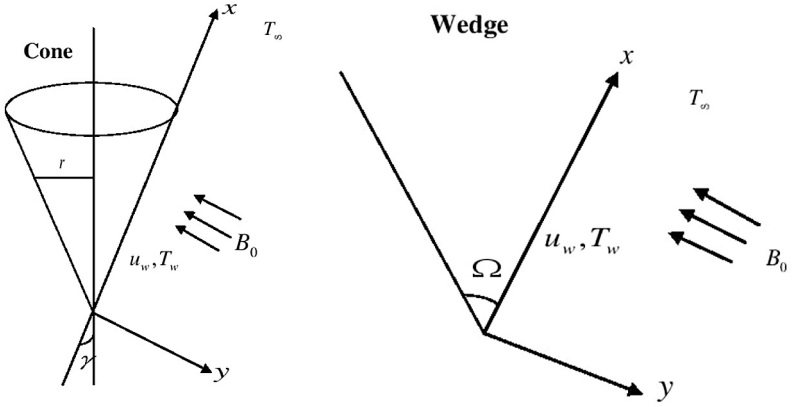


**Figure 1** Geometrical configuration of the flow.

$$\frac{\partial^3 f}{\partial \zeta^3}+(m+1)f\frac{\partial^2 f}{\partial \zeta^2}-\left(\frac{\partial f}{\partial \zeta}\right)^2-M\frac{\partial f}{\partial \zeta}+Gr\theta\cos\gamma=0, \tag{7}$$

$$\frac{\partial^2\theta}{\partial\zeta^2}-Pr\beta\left[\begin{array}{l}s\left(\left(\frac{\partial f}{\partial\zeta}\right)^2\theta-(m+1)f\frac{\partial^2 f}{\partial\zeta^2}\theta-2(m+1)f\frac{\partial f}{\partial\zeta}\frac{\partial\theta}{\partial\zeta}+(s-1)\left(\frac{\partial f}{\partial\zeta}\right)^2\theta\right)\\+(m+1)^2\left(f^2\frac{\partial^2\theta}{\partial\zeta^2}+f\frac{\partial f}{\partial\zeta}\frac{\partial\theta}{\partial\zeta}\right)\end{array}\right]\\+Pr\left((m+1)f\frac{\partial\theta}{\partial\zeta}-s\frac{\partial f}{\partial\zeta}\theta\right)+\left(A^*\frac{\partial f}{\partial\zeta}+B^*\theta\right)=0, \tag{8}$$

The relevant boundary conditions are

$$\left.\begin{array}{lll}f=0, & \frac{\partial f}{\partial\zeta}=1, & \theta=1, \quad \text{at } \zeta=0,\\ \frac{\partial f}{\partial\zeta}=0, & \theta=0, & \text{as } \zeta\to\infty,\end{array}\right\} \tag{9}$$

In Eqs. (7) and (8) $M$ is the magnetic field parameter, $Gr$ is the thermal Grashof number, $Pr$ is the Prandtl number, $\beta$ is the thermal relaxation parameter, and these are given by,

$$M=\frac{\sigma_0 B_0^2 l^2}{\rho\upsilon}, \quad Gr=\frac{l^2 g\beta_T(T_w-T_\infty)}{\upsilon u_w}, \quad Pr=\frac{\mu c_p}{k}, \quad \beta=\frac{\delta\upsilon}{l^2}, \tag{10}$$

The physical quantities in view of many engineering and industrial applications are friction factor ($C_f$) and local Nusselt number ($Nu$). These are defined as,

$$C_f=\frac{C_f^*}{\mu u_w}=f''(0), \quad Nu=\frac{hl}{k(T_w-T_\infty)}=-\theta'(0), \tag{11}$$

where $C_f^*$ is the dimensional wall shear stress.

## 3. Results and discussion

The set of nonlinear differential Eqs. (7) and (8) with the associated boundary conditions is solved via R.K. and Newton's methods. The impact of pertinent parameters namely, mag-

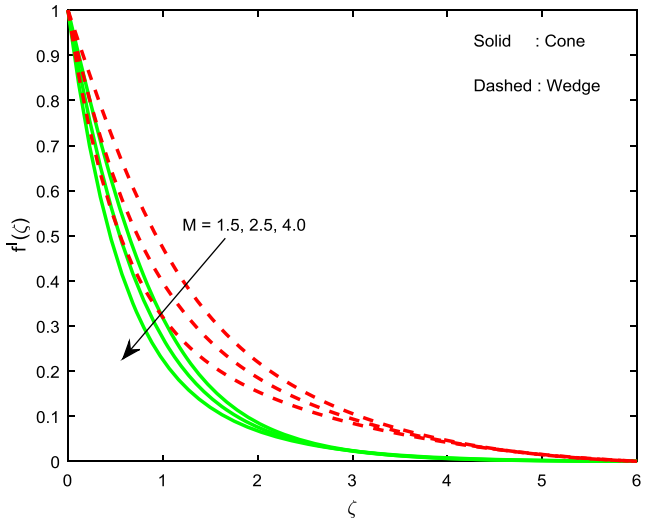


**Figure 2** Velocity behaviour with varying magnetic field parameter ($M$).

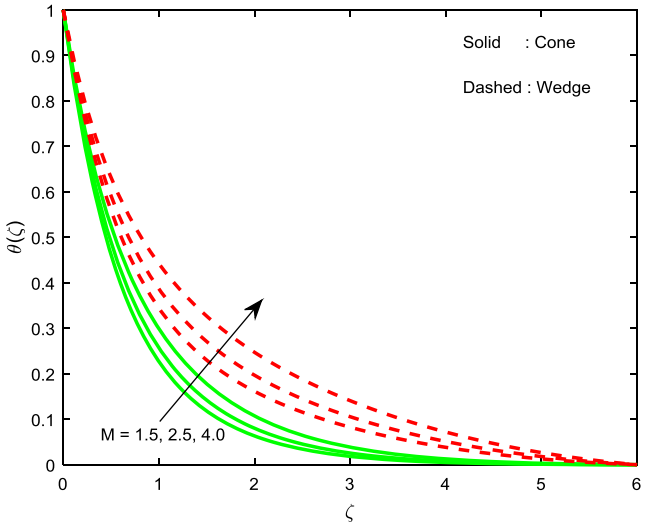


**Figure 3** Temperature behaviour with varying magnetic field parameter ($M$).

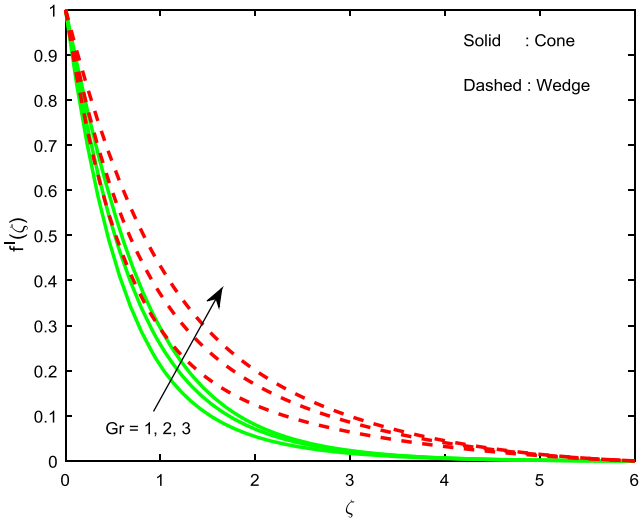


**Figure 4** Velocity behaviour with varying thermal Grashof number ($Gr$).

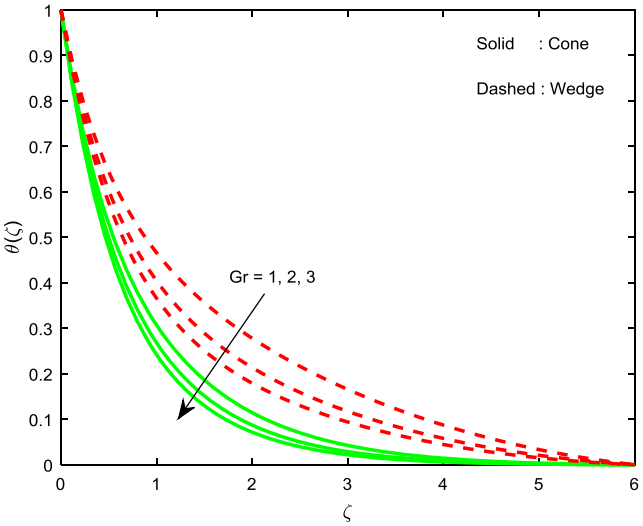


**Figure 5** Temperature behaviour with varying thermal Grashof number ($Gr$).

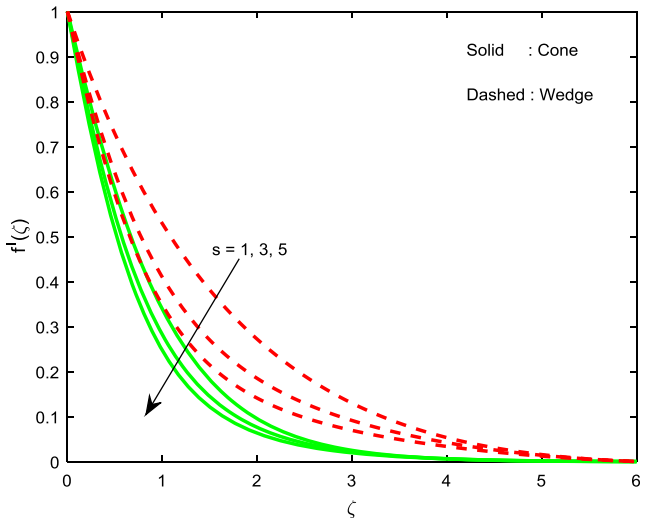


**Figure 6** Velocity behaviour with varying wall temperature parameter ($s$).

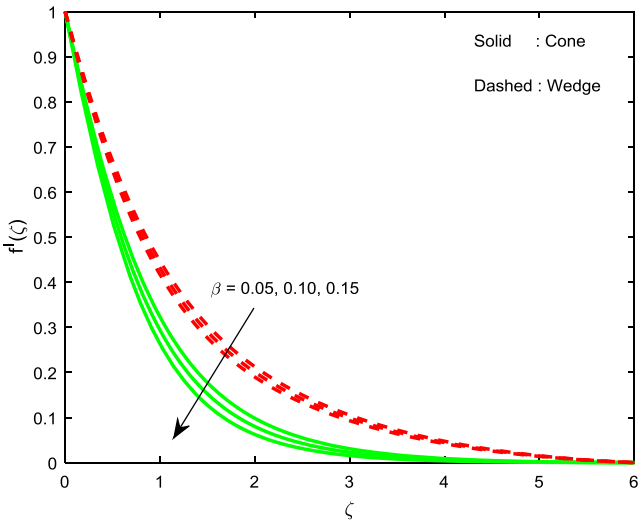


**Figure 8** Velocity behaviour with varying thermal relaxation parameter ($\beta$).

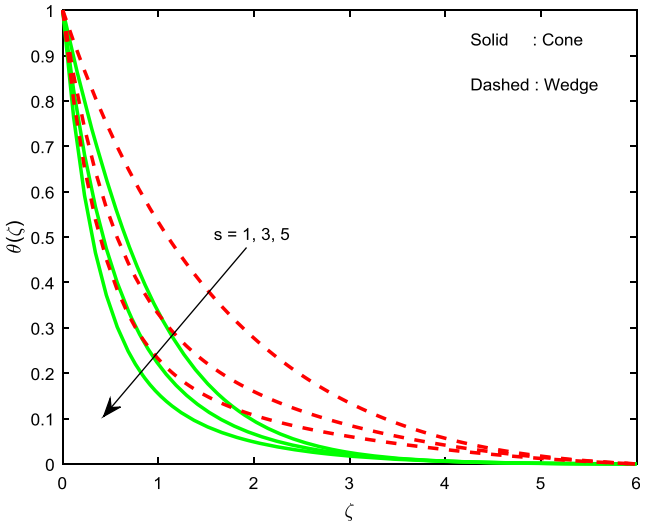


**Figure 7** Temperature behaviour with varying wall temperature parameter ($s$).

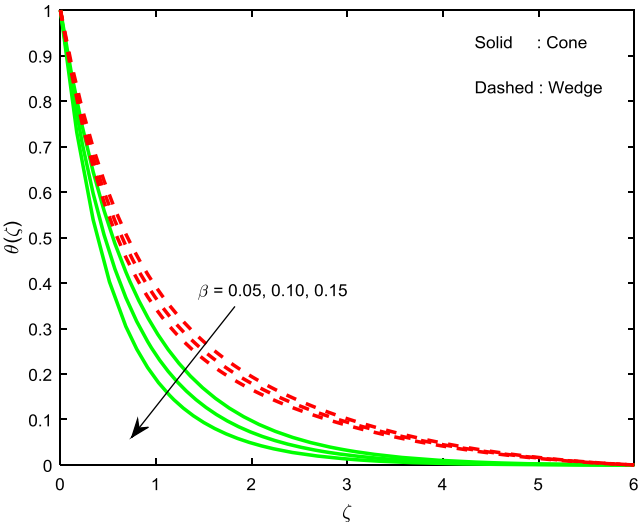


**Figure 9** Temperature behaviour with varying thermal relaxation parameter ($\beta$).

netic field parameter ($M$), thermal Grashof number ($Gr$), wall temperature parameter ($s$), thermal relaxation parameter ($\beta$), Prandtl number ($Pr$) and non-uniform heat parameters ($A^*$ and $B^*$) on the flow field along with the wall friction factor and heat transfer coefficient, are presented in the form of graphical and tabulated results. We considered the values of dimensionless parameters as $Pr = 0.7$, $M = 2$, $Gr = 3$, $s = 2.5$, $\beta = 0.1$ and $A^* = B^* = 0.2$. These values have been taken as common for the complete study unless otherwise specified in the figures and tables.

Figs. 2 and 3 demonstrate the effect of magnetic field parameter ($M$) on dimensionless fluid velocity and temperature distributions. From Fig. 2, we found that accelerating values of magnetic field parameter ($M$) decay the velocity profiles. But an opposite trend is perceived in fluid temperature through Fig. 3. Physically, increasing values of $M$ create Lorentz force in the flow, which has the tendency to restrict the fluid motion. This force also generates heat energy in the flow. Therefore the thermal boundary layer thickness becomes bigger. Moreover, we notice that the magnetic field parameter effectively reduces the fluid velocity on the flow past a cone than that of wedge.

The nature of velocity and temperature distributions with variable values of thermal Grashof number ($Gr$) can be visualized through Figs. 4 and 5 respectively. In Fig. 4, we observe that fluid velocity is an increasing function of $Gr$ but an opposite outcome is observed in temperature profiles. We know that Grashof number is the ratio of the buoyancy force to the viscous force. So, an overshoot in the momentum boundary layer thickness is noticed. Figs. 6 and 7 are sketched to study the impact of wall temperature parameter ($s$) on dimensionless velocity and temperature fields. A deterioration in both velocity and temperature fields can be observed with the larger the values of $s$. This agrees with the results given by Ouaf [14]. It is worth to mention that the temperature profiles of the flow over

Please cite this article in press as: K. Anantha Kumar et al., Magnetohydrodynamic Cattaneo-Christov flow past a cone and a wedge with variable heat source/sink, Alexandria Eng. J. (2016), http://dx.doi.org/10.1016/j.aej.2016.11.013

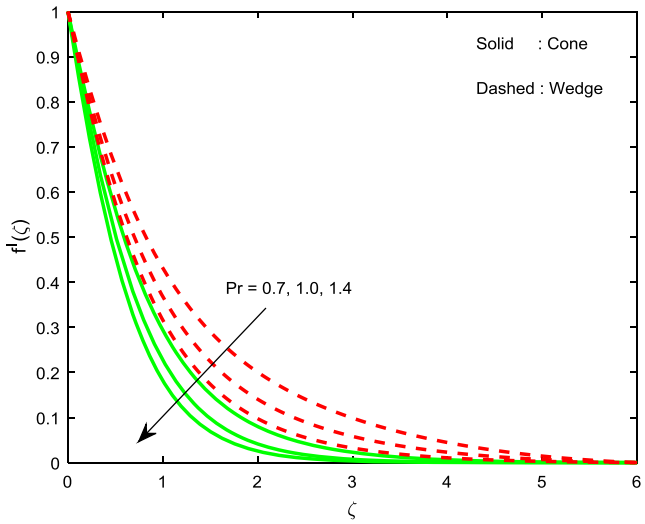


**Figure 10** Velocity behaviour with varying Prandtl number ($Pr$).

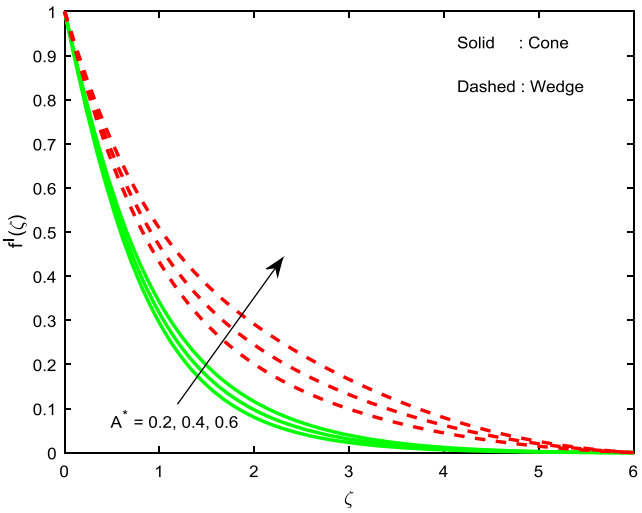


**Figure 12** Velocity behaviour with varying non-uniform heat source/sink parameter ($A^*$) when $B^* = 0.2$ (i.e. $A^*, B^* > 0$).

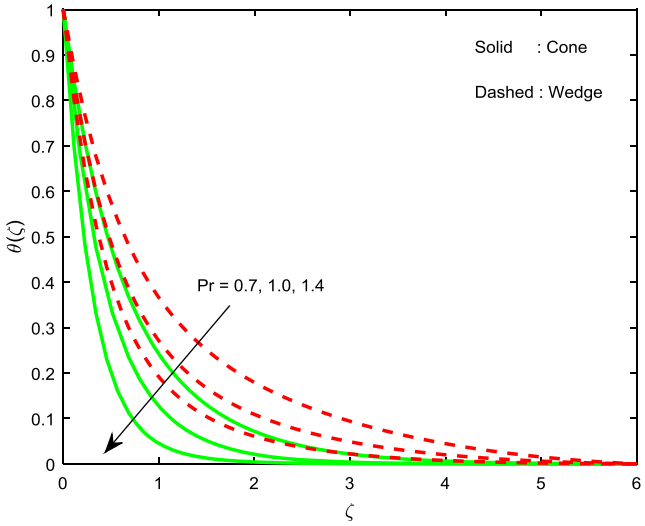


**Figure 11** Temperature behaviour with varying Prandtl number ($Pr$).

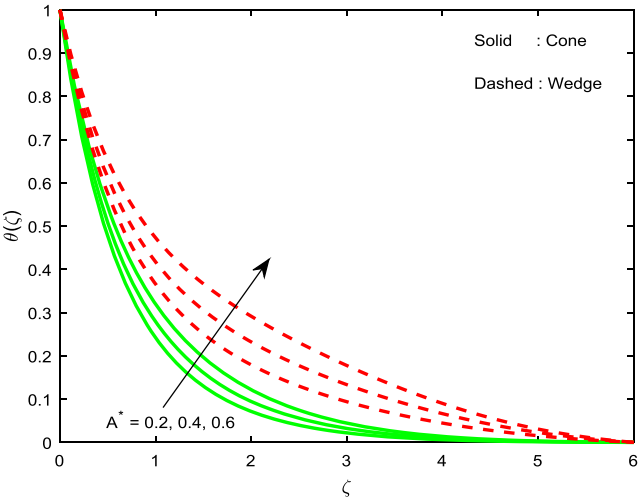


**Figure 13** Temperature behaviour with varying non-uniform heat source/sink parameter ($A^*$) when $B^* = 0.2$ (i.e. $A^*, B^* > 0$).

a wedge are not much affected while compared with the flow over a cone.

Figs. 8 and 9 exhibit the effect of thermal relaxation parameter ($\beta$) on velocity and temperature profiles. Both velocity and temperature overshoot are noted with an increase in $\beta$. The physical reason for such results is that as we hike the values of $\beta$ fluid particles exhibit non-conducting behaviour due to which they require more time to bring the heat to their surrounding particles. The influence of Prandtl number ($Pr$) on velocity and temperature is shown in Figs. 10 and 11 respectively. Since the Prandtl number is inversely proportional to the thermal diffusivity, both the velocity and temperature profiles are found to be decreased.

Figs. 12–15 are plotted to analyse the effect of non-uniform heat source or sink parameters ($A^*, B^*$) on velocity and temperature distributions. Figs. 12 and 13 enable us to say that boosting the values of $A^*$ heightens the fluid velocity and temperature. But we notice a reverse trend from Figs. 14 and 15 for increasing values of $B^*$ negatively. (Here we have taken $A^* = -0.2$.) As we discussed earlier, the values $A^*, B^* > 0$ correspond to generation of heat in the fluid and $A^*, B^* < 0$ leads to an absorption of heat from the flow.

Table 1 illustrates the influence of few physical dimensionless parameters on wall friction factor ($f''(0)$) and reduced heat transfer coefficient ($-\theta'(0)$) for the flow past a wedge and a cone. It is obvious that a rise in the magnetic field parameter lessens both skin friction and heat transfer rate. Meanwhile elevating the values of thermal Grashof number causes an enhancement in both heat transfer coefficient and wall friction factor. It is also examined that Nusselt number increases with wall temperature and thermal relaxation parameters. Heat generation (or absorption) caused by non-uniform heat source/sink parameters enhances (or reduces) the friction factor and same kind of behaviour is repeated for heat transfer coefficient. Validation of the present results with published results are depicted in Table 2.

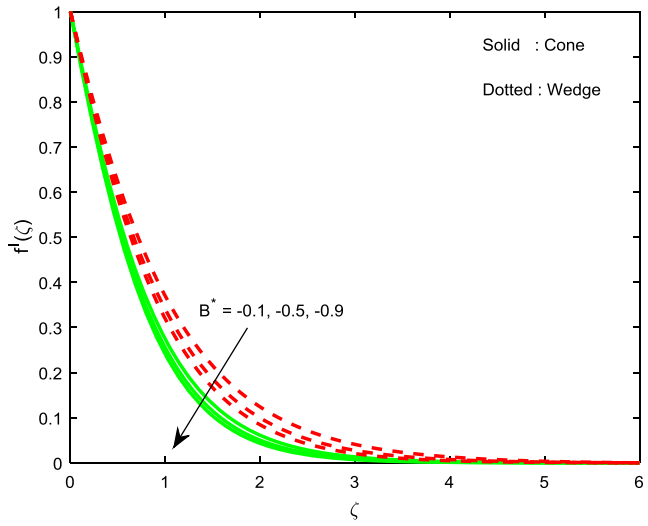


**Figure 14** Velocity behaviour with varying non-uniform heat source/sink parameter ($B^*$) when $A^* = -0.2$ (i.e. $A^*, B^* < 0$).

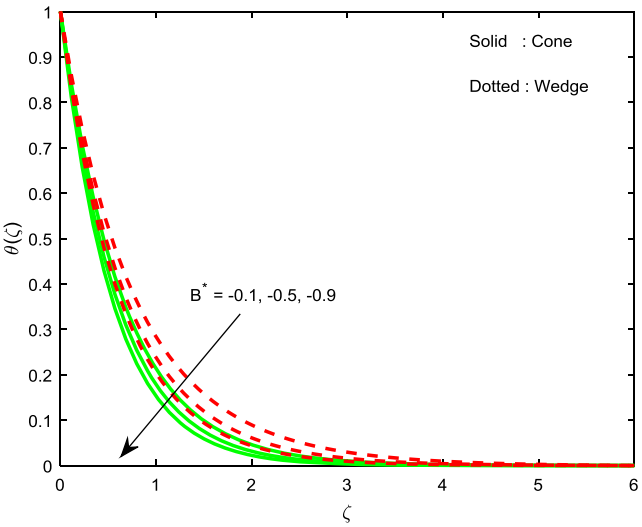


**Figure 15** Temperature behaviour with varying uniform heat source/sink parameter ($B^*$) profiles when $A^* = -0.2$ (i.e. $A^*, B^* < 0$).

**Table 1** Influence of various physical parameters on friction factor ($f''(0)$) and heat transfer coefficient ($-\theta'(0)$).

| $M$ | $Gr$ | $s$ | $\beta$ | $Pr$ | $A^*$ | $B^*$ | $f''(0)$ | | $-\theta'(0)$ | |
|---|---|---|---|---|---|---|---|---|---|---|
| | | | | | | | Cone | Wedge | Cone | Wedge |
| 1.5 | | | | | | | −0.8740 | −0.6244 | 1.577 | 1.2598 |
| 2.5 | | | | | | | −1.1778 | −0.9669 | 1.5044 | 1.1795 |
| 4.0 | | | | | | | −1.5708 | −1.3984 | 1.4085 | 1.0786 |
| | 1.0 | | | | | | −1.538 | −1.3842 | 1.4008 | 1.0522 |
| | 2.0 | | | | | | −1.2764 | −1.0830 | 1.4793 | 1.1489 |
| | 3.0 | | | | | | −1.0311 | −0.8027 | 1.5398 | 1.2181 |
| | | 1.0 | | | | | −0.9112 | −0.6339 | 0.9455 | 0.6290 |
| | | 3.0 | | | | | −1.0631 | −0.08432 | 1.7233 | 1.3881 |
| | | 5.0 | | | | | −1.1669 | −0.9676 | 2.4192 | 2.0133 |
| | | | 0.05 | | | | −0.9715 | −0.7758 | 1.3083 | 1.1171 |
| | | | 0.1 | | | | −1.0311 | −0.8027 | 1.5398 | 1.2181 |
| | | | 0.15 | | | | −1.0993 | −0.8286 | 1.8426 | 1.3206 |
| | | | | 0.7 | | | −1.0311 | −0.8027 | 1.5398 | 1.218 |
| | | | | 1.0 | | | −1.1751 | −0.9059 | 2.1702 | 1.5828 |
| | | | | 1.38 | | | −1.3191 | −1.0009 | 3.1290 | 1.9916 |
| | | | | | 0.2 | | −1.0311 | −0.8027 | 1.5398 | 1.2181 |
| | | | | | 0.4 | | −0.9919 | −0.7538 | 1.4205 | 1.1042 |
| | | | | | 0.6 | | −0.9496 | −0.7015 | 1.2957 | 0.9846 |
| | | | | | | −0.1 | −1.1301 | −0.9251 | 1.8927 | 1.5495 |
| | | | | | | −0.5 | −1.1636 | −0.9660 | 2.0492 | 1.6953 |
| | | | | | | −0.9 | −1.1908 | −0.9990 | 2.1921 | 1.8273 |

**Table 2** Comparison of the present work with Palani et al. [52].

| $Pr$ | $C_f$ | | $Nu$ | |
|---|---|---|---|---|
| | Palani et al. [52] | Current study | Palani et al. [52] | Current study |
| 0.1 | 1.10236 | 1.10235 | 0.20922 | 0.20922 |
| 0.7 | 0.82566 | 0.82567 | 0.44771 | 0.44770 |
| 1.0 | 0.77524 | 0.77524 | 0.50670 | 0.50671 |

Please cite this article in press as: K. Anantha Kumar et al., Magnetohydrodynamic Cattaneo-Christov flow past a cone and a wedge with variable heat source/sink, Alexandria Eng. J. (2016), http://dx.doi.org/10.1016/j.aej.2016.11.013

## 4. Concluding remarks

This article reports the flow and heat transfer behaviour of MHD flow over a cone and a wedge with Cattaneo-Christov heat flux model. The influence of non-uniform heat source or sink is also contemplated. The boundary value problem was solved numerically via R.-K. and Newton's methods. The foremost results have been listed below:

- Momentum boundary layer thickness is large on the flow past a wedge when compared with the flow past a cone.
- The heat transfer rate of the flow past a cone is higher than that of the wedge flow.
- Prandtl number has propensity to inflate the Nusselt number effectively.
- Rising values of thermal relaxation parameter magnify the heat transfer performance.
- Heat generation (absorption) caused by $A^*, B^*$ regulates the temperature field.

## References

[1] W.E. Stewart, R. Prober, Heat transfer and diffusion in wedge flows with rapid mass transfer, Int. J. Heat Mass Transfer 5 (12) (1962) 1149–1163.
[2] H.T. Lin, L.K. Lin, Similarity solutions for laminar forced convection heat transfer from wedges to fluids of any Prandtl number, Int. J. Heat Mass Transfer 30 (6) (1987) 1111–1118.
[3] K. Vajravelu, J. Nayfeh, Hydromagnetic convection at a cone and a wedge, Int. Commun. Heat Mass Transfer 19 (5) (1992) 701–710.
[4] A.J. Chamkha, Non-Darcy hydromagnetic free convection from a cone and a wedge in porous medium, Int. Commun. Heat Mass Transfer 23 (6) (1996) 875–887.
[5] C.H. Hsu, C.S. Chen, J.T. Teng, Temperature and flow fields for the flow of a second grade fluid past a wedge, Int. J. Nonlinear Mech. 32 (5) (1997) 933–946.
[6] K.A. Yih, Uniform suction/blowing effects on forced convection about a wedge: uniform heat flux, Acta Mech. 128 (1998) 173–181.
[7] M. Kumari, MHD flow over a wedge with large blowing rates, Int. J. Eng. Sci. 36 (3) (1998) 299–314.
[8] M. Kumari, H.S. Takhar, G. Nath, Mixed convection flow over a vertical wedge embedded in a highly porous medium, Heat Mass Transfer 37 (2–3) (2001) 139–146.
[9] M. Massoudi, Local non-similarity solutions for the flow of a non-Newtonian fluid over a wedge, Int. J. Non-linear Mech. 36 (6) (2001) 961–976.
[10] S.P.A. Devi, R. Kandasamy, Effect of chemical reaction, heat and mass transfer on non-linear MHD laminar boundary layer flow over a wedge with suction or injection, Int. Commun. Heat Mass Transfer 29 (5) (2002) 707–716.
[11] W.T. Cheng, H.T. Lin, Non-similarity solution and correlation of transient heat transfer in laminar boundary layer flow over a wedge, Int. J. Eng. Sci. 40 (5) (2002) 531–548.
[12] Y.J. Kim, Heat and mass transfer in MHD micropolar flow on a vertical moving porous plate in a porous medium, Transp. Porous Media 56 (1) (2004) 17–37.
[13] R. Kandasamy, K. Periasamy, K.K.S. Prabhu, Effects of chemical reaction, heat and mass transfer along a wedge with heat source and concentration in the presence of suction or injection, Int. J. Heat Mass Transfer 48 (7) (2005) 1388–1394.
[14] M.E. Ouaf, Exact solution of thermal radiation on MHD flow over a stretching porous sheet, Appl. Math. Comput. 170 (2) (2005) 1117–1125.
[15] M.A. Hossain, S. Bhowmick, R.S.R. Gorla, Unsteady mixed-convection boundary layer flow along a symmetric wedge with variable surface temperature, Int. J. Eng. Sci. 44 (10) (2006) 607–620.
[16] S.M.M. El-Kabeir, M. Modather, M. Abdou, Chemical reaction, heat and mass transfer on MHD flow over a vertical isothermal cone surface in micropolar fluids with heat generation/absorption, Appl. Math. Sci. 1 (34) (2007) 1663–1674.
[17] B. Yao, Approximate analytical solution to the Falkner-Skan wedge flow with the permeable wall of uniform suction, Commun. Nonlinear Sci. Numer. Simul. 14 (8) (2009) 3320–3326.
[18] T. Hayat, M. Hussain, S. Nadeem, S. Mesloub, Falkner-Skan wedge flow of a power-law fluid with mixed convection and porous medium, Comput. Fluids 49 (1) (2011) 22–28.
[19] A. Postelnicu, I. Pop, Falkner-Skan boundary layer flow of a power-law fluid past a stretching wedge, Appl. Math. Comput. 217 (9) (2011) 4359–4368.
[20] M.A. Seddeek, A.A. Afify, A.M.A. Hanaya, Similarity solutions for a steady MHD Falkner-Skan flow and heat transfer over a wedge considering the effects of variable viscosity and thermal conductivity, Appl. Appl. Math. 4 (2) (2009) 301–313.
[21] N.A. Yacob, A. Ishak, I. Pop, Falkner-Skan problem for a static or moving wedge in nanofluids, Int. J. Therm. Sci. 50 (2) (2011) 133–139.
[22] A.M. Rashad, A.Y. Bakier, MHD effects on non-Darcy forced convection boundary layer flow past a permeable wedge in a porous medium with uniform heat flux, Nonlinear Anal.: Model. Control 14 (2) (2009) 249–261.
[23] K. Atalik, U. Sonmezler, Heat transfer enhancement for boundary layer flow over a wedge by the use of electric fields, Appl. Math. Model. 35 (9) (2011) 4516–4525.
[24] K.L. Hsiao, MHD mixed convection for viscoelastic fluid past a porous wedge, Int. J. Nonlinear Mech. 46 (1) (2011) 1–8.
[25] M.M. Rahman, M.A.A. Lawatia, I.A. Eltayeb, N.A. Salti, Hydromagnetic slip flow of water based nanofluids past a wedge with convective surface in the presence of heat generation or absorption, Int. J. Therm. Sci. 57 (2012) 172–182.
[26] M.S. Khan, I. Karim, M.S. Islam, M. Wahiduzzaman, MHD boundary layer radiative, heat generating and chemical reacting flow past a wedge moving in a nanofluid, Nano Convergence 1 (1) (2014) 1–13.
[27] R. Kandasamy, I. Muhaimin, A.K. Rosmila, The performance evaluation of unsteady MHD non-Darcy nanofluid flow over a porous wedge due to renewable (solar) energy, Renew. Energy 64 (2014) 1–9.
[28] M.M. Rashidi, M. Ali, N. Feridoonimehr, B. Rostami, M.A. Hossain, Mixed convection heat transfer for MHD viscoelastic fluid flow over a porous wedge with thermal radiation, Adv. Mech. Eng. 6 (2014) (2014) 735939.
[29] M.R. Kasmani, S. Sivasankaran, M. Bhuvaneswari, Z. Siri, Effect of chemical reaction on convective heat transfer of boundary layer flow in nanofluid over a wedge with heat generation/absorption and suction, J. Appl. Fluid Mech. 9 (1) (2016) 379–388.
[30] J.V. Ramana Reddy, V. Sugunamma, N. Sandeep, K. Anantha Kumar, Influence of non-uniform heat source/sink on MHD Nano fluid flow past a slendering stretching sheet with slip effects, Global J. Pure Appl. Math. 12 (1) (2016) 247–254.
[31] D. Mathili, R. Sivaraj, M.M. Rashidi, Z. Yang, Casson fluid flow over a vertical cone with non-uniform heat source/sink and higher order chemical reaction, J. Naval Arch. Mar. Eng. 15 (2015) 125–136.

Please cite this article in press as: K. Anantha Kumar et al., Magnetohydrodynamic Cattaneo-Christov flow past a cone and a wedge with variable heat source/sink, Alexandria Eng. J. (2016), http://dx.doi.org/10.1016/j.aej.2016.11.013

[32] M.J. Babu, N. Sandeep, C.S.K. Raju, Heat and mass transfer in MHD Eyring-Powell nanofluid flow due to cone in porous medium, Int. J. Eng. Res. Afr. 19 (2016) 57–74.
[33] C.S.K. Raju, N. Sandeep, Dual solutions for unsteady heat and mass transfer in bio-convection flow towards a rotating cone/plate in a rotating fluid, Int. J. Eng. Res. Afr. 20 (2016) 161–176.
[34] S.M.A. Harbi, Numerical study of natural convection heat transfer with variable viscosity and thermal radiation from a cone and wedge in porous medium, Appl. Math. Comput. 170 (2005) 64–75.
[35] J.B.J. Fourier, Theorie Analytique De La Chaleur, Paris, 1822.
[36] C. Cattaneo, Sulla conduzione del calore, Atti Semin. Mat. Fis. Univ. Modena Reggio Emilia 3 (1948) 83–101.
[37] C.I. Christov, On frame indifferent formulation of the Maxwell-Cattaneo model of finite speed heat conduction, Mech. Res. Commun. 36 (2009) 481–486.
[38] S. Han, L. Zheng, C. Li, X. Zhang, Coupled flow and heat transfer in viscoelastic fluid with Cattaneo-Christov heat flux model, Appl. Math. Lett. 38 (2014) 87–93.
[39] T. Hayat, T. Muhammad, A. Alsaedi, M. Mustafa, A comparative study for flow of viscoelastic fluids with Cattaneo-Christov heat flux, PLoS ONE 11 (5) (2016) e0155185.
[40] M. Mustafa, Cattaneo-Christov heat flux model for rotating flow and heat transfer of upper-convected Maxwell fluid, AIP Adv. 5 (4) (2015) 047109.
[41] T. Hayat, S. Qayyum, M. Imtiaz, A. Alsaedi, Impact of Cattaneo-Christov heat flux in Jeffrey fluid flow with homogeneous-heterogeneous reactions, PLoS ONE 11 (2) (2016) e0148662.
[42] M. Waqas, T. Hayat, M. Farooq, S.A. Shehzad, A. Alsaedi, Cattaneo-Christov heat flux model for flow of variable thermal conductivity generalized Burgers fluid, J. Mol. Liq. 220 (2016) 642–648.
[43] S. Shah, S. Hussain, M. Sagheer, MHD effects and heat transfer for the UCM fluid along with Joule heating and thermal radiation using Cattaneo-Christov heat flux model, AIP Adv. 6 (2016) Article Id: 085103.
[44] M.Y. Malik, M. Khan, T. Salahuddin, I. Khan, Variable viscosity and MHD flows in Casson fluid with Cattaneo-Christov heat flux model: using Keller box method, Eng. Sci. Tech.: Int. J. (2016), http://dx.doi.org/10.1016/j.jestch.2016.06.008.
[45] T. Salahuddin, M.Y. Malik, A. Hussain, S. Bilal, M. Awais, MHD flow of Cattaneo-Christov heat flux model for Williamson fluid over a stretching sheet with variable thickness: using numerical approach, J. Magn. Magn. Mater. 401 (2016) 991–997.
[46] J. Li, L. Zheng, L. Liu, MHD Viscoelastic flow and heat transfer over a vertical stretching sheet with Cattaneo-Christov heat flux effects, J. Mol. Liq. 221 (2016) 19–25.
[47] S.A. Shehzad, F.M. Abbasi, T. Hayat, A. Alsaedi, Cattaneo-Christov heat flux model for Darcy-Forchheimer flow of an Oldroyd-B fluid with variable conductivity and non-linear convection, J. Mol. Liq. 224 (2016) 274–278.
[48] F.M. Abbasi, S.A. Shehzad, Heat transfer analysis for three-dimensional flow of Maxwell fluid with temperature dependent thermal conductivity: application of Cattaneo–Christov heat flux model, J. Mol. Liq. 220 (2016) 848–854.
[49] F.M. Abbasi, S.A. Shehzad, T. Hayat, A. Alsaedi, Influence of Cattaneo-Christov heat flux in flow of an Oldroyd-B fluid with variable thermal conductivity, Int. J. Numer. Meth. Heat Fluid Flow 26 (2016) 2271–2282.
[50] F.M. Abbasi, M. Mustafa, S.A. Shehzad, M.S. Alhuthali, T. Hayat, Analytical study of Cattaneo-Christov heat flux model for a boundary layer flow of Oldroyd-B fluid, Chin. Phys. B 25 (2015) Article Id: 014701.
[51] S.A. Shehzad, F.M. Abbasi, T. Hayat, B. Ahmad, Cattaneo-Christov heat flux model for third-grade fluid flow towards exponentially stretching sheet, Appl. Math. Mech. 37 (2016) 761–768.
[52] G. Palani, E.J.L. Kumar, K.Y. Kim, Free convection effects on a vertical cone with variable viscosity and thermal conductivity, J. Appl. Mech. Tech. Phys. 57 (2016) 473–482.

Please cite this article in press as: K. Anantha Kumar et al., Magnetohydrodynamic Cattaneo-Christov flow past a cone and a wedge with variable heat source/sink, Alexandria Eng. J. (2016), http://dx.doi.org/10.1016/j.aej.2016.11.013